Luminosity measurements at LHCb using dimuon pairs produced via elastic two photon fusion

LHCb-2008-001
16/03/2010

LHCb Public Note

Issue: 1
Revision: 0
Reference: LHCb-2008-001
Created: October 24, 2007
Last modified: March 5, 2010

Prepared by: J. Anderson[1], R. McNulty[2]

[1] *Physik-Institut der Universität Zürich*
[2] *University College Dublin*

Abstract

This note outlines the feasibility of using the elastic two photon process $pp \to p + \mu^+\mu^- + p$ to make luminosity measurements at LHCb. The overall efficiency at LHCb for recording and selecting $pp \to p + \mu^+\mu^- + p$ events produced within $1.6 < \eta < 5$ has been determined using Monte-Carlo to be 0.0587 ± 0.0008, yielding 5210 ± 71(stat.) events for an integrated luminosity of 1 fb^{-1}. The main background processes where dimuons are produced via inelastic two-photon fusion and double Pomeron exchange have been studied using the full LHCb detector simulation while the other background sources, including backgrounds caused by K/π mis-identification, have been studied at four vector level. The background is estimated to be $(4.1 \pm 0.5(\text{stat.}) \pm 0.6(\text{syst.}))\%$ of the signal level. Most of this background comes from K/π mis-identification, although the largest source of uncertainty in the estimation is due to knowledge of the number of events produced via double Pomeron exchange. Systematic uncertainties on a luminosity measurement at LHCb using this channel are estimated to be $\sim$1% the largest of which are the uncertainty on the predicted cross-section for events containing dimuons produced via double Pomeron exchange, and the knowledge of the trigger and reconstruction efficiency for muons in LHCb.

Contents

1 Introduction

The measurement of a cross-section, σ, within a fiducial volume v is given by $\sigma(v) = N/(\varepsilon\mathcal{L})$ where N is the number of events observed, ε is the efficiency for recording those events and $\mathcal{L}$ is the integrated luminosity. Knowledge of the integrated luminosity is therefore required to make any cross-section measurement. In general there are three methods for determining the absolute luminosity at a colliding beam experiment:

1. A simultaneous measurement of a pair of cross-sections that are connected with each other quadratically via the optical theorem. A well known example of this is the measurement of the total inelastic cross-section and the elastic cross-section at very high pseudorapidities $|\eta| \simeq 9$ (see for example [1]). While such a measurement will be made at the central general purpose LHC detectors, ATLAS and CMS/TOTEM, which have dedicated forward detectors for this purpose, it is not a viable technique at LHCb as the detector instrumentation only extends up to $\eta = 4.9$.

2. Direct measurement of the beam currents and shapes. While the beam currents can be accurately determined using beam transformers the beam profiles are more difficult to determine directly and usually constitute the dominant source of uncertainty on a luminosity measurement using this technique. There are a number of traditional methods for determining the beam profile, for example the Van Der Meer scan method [2] where the colliding beams are moved transversely across each other and the wire scan method [3] where the profiles are measured by passing wires through the beams. Luminosity measurements at the LHC experiments based on these traditional techniques are expected to have associated uncertainties of $\sim 10\%$. A more recently proposed method [4] for determining the beam profiles at colliding beam experiments utilises the precision vertex detectors found at modern HEP experiments to reconstruct beam gas interactions near the beams' crossing point. This method, which will be implemented at LHCb, is currently under investigation and is expected to result in a luminosity measurement with an associated uncertainty of $\sim$1 - 3%.

3. Finally, another way to measure the luminosity is to record the event rate of a process with a cross-section that can be accurately calculated from theory. The accuracy of a luminosity measurement using this method is usually limited by the theoretical uncertainty on the calculated cross-section. Two candidate proccesses have been identified for such a measurement at LHCb: $W^{\pm}$ and Z production which has been investigated previously [5, 6, 7] and is expected to yield a luminosity measurement with a $\sim$4% uncertainty due to uncertainties in our understanding of the proton Parton Distribution Functions (PDFs); and elastic $\mu^+\mu^-$ pair production via two-photon fusion, $pp \rightarrow p + \mu^+\mu^- + p$, which has a cross-section which is better known with a theoretical uncertainty of $< 1\%$ [8] but has a much lower event rate. This note builds on the work of A. Shamov and V. Telnov [9] and outlines the progress that has been made towards making a luminosity measurement at LHCb using the event rate of this second process.

Knowing the cross-section for elastic $\mu^+\mu^-$ pair production via two-photon fusion, $\sigma_{el}(v)$, within some fiducial volume v, the absolute luminosity for a given data set at LHCb can be calculated from

$$\int \mathcal{L}dt = \frac{N_{el}^{obs} - N_{el}^{back}}{\varepsilon_{el}^{total} \cdot \sigma_{el}(v)} \tag{1}$$

Where N_{el}^{obs} is the number of observed $pp \to p + \mu^+\mu^- + p$ candidate events, N_{el}^{back} is the expected number of background events and ε_{el}^{total} is the total efficiency at LHCb for recording $pp \to p + \mu^+\mu^- + p$ events produced within the volume v. The total efficiency can be expressed as the product

$$\varepsilon_{el}^{total} = A_{el}^{geom} \times A_{el}^{kin} \times \varepsilon_{el}^{trigger} \times \varepsilon_{el}^{reco} \tag{2}$$

where A_{el}^{geom} and A_{el}^{kin} are the acceptances due to the detector topology and offline kinematic selection criteria respectively, while $\varepsilon_{el}^{trigger}$ and ε_{el}^{reco} are the trigger and reconstruction efficiencies.

This note presents Monte-Carlo based estimates of the acceptances, efficiencies and level of background for the $pp \to p + \mu^+\mu^- + p$ channel at LHCb and is organised as follows: in Section 2 we briefly review dimuon production via two photon fusion and discuss the uncertainty on cross-section predictions for this process; in Section 3 we outline the event characteristics and experimental efficiency of $pp \to p + \mu^+\mu^- + p$ events at LHCb, in addition we outline a new L0 dimuon trigger stream designed to improve the trigger efficiency for these events; section 4 describes the various background processes; in Section 5 a set of offline selection cuts are proposed and their effects on both the signal and background events are described; in Section 6 we discuss a possible method that will enable the effects of multiple interaction bunch crossings to be determined; finally, in section 7 we discuss the expected systematic and statistical uncertainties on the proposed luminosity measurement.

2 Accuracy of predicted cross-section

In this section we give a brief review of dimuon production via two-photon fusion and discuss the accuracy of current cross-section predictions for this process. For more complete discussions see [8], [9] and [10].

2.1 Elastic $\mu^+\mu^-$ production via photon fusion

Within the Effective Photon Approximation (EPA) the two-photon muon pair production cross-section at the LHC can be calculated as a convolution of the direct cross-section of two colliding photons that produce a muon pair and the fluxes of virtual photons, dn_1 and dn_2, surrounding the two colliding protons

$$d\sigma = \sigma_{\gamma\gamma \to \mu^+\mu^-} dn_1 dn_2 \tag{3}$$

For elastic events where the impact parameter of the colliding protons is large the protons essentially behave as point-like particles and the virtual photon fluxes, dn_1 and dn_2, will be equal to

$$dn_{QED} = \frac{\alpha}{\pi}\frac{d\omega}{\omega}\frac{dq^2}{q^2}\left(1 - \frac{q_{min}^2}{q^2}\right) = \frac{\alpha}{\pi}\frac{d\omega}{\omega}\frac{\vec{q}_T d\vec{q}_T^2}{(\omega^2/\gamma^2 + \vec{q}_T^2)^2} \tag{4}$$

where $q(\omega, \vec{q})$ is the four-momentum of the photon, $\gamma = E/m_p$ is the Lorentz factor of the colliding proton and m_p is the mass of the proton. Here the process is only sensitive to the proton mass, charge and anomalous magnetic moment which are known very accurately with measurement uncertainties below 0.001%. However, when the impact parameters are smaller the process is sensitive to the protons electric and magnetic form factors G_E and G_M and the virtual photon fluxes are given by

$$dn_{elastic} = dn_{QED}\frac{G_E^2 - q^2/(2m_p G_M)^2}{1 - (q/2m_p)^2} \tag{5}$$

The protons electromagnetic form factors have been measured at SLAC [11] with an uncertainty of $\sim$2%. The predicted cross-section for elastic collisions of the type illustrated in Figure 1(a) will have contributions from both the point-like process and the process that is sensitive to the electromagnetic form factors . In order for the predicted elastic cross-section to have an associated uncertainty below 1% the event rate of the process that is sensitive to the electromagnetic form factors must be below 50% of the total event rate. This can be achieved by selecting events that have small dimuon pair transverse momenta ($P_T^{\mu\mu}$) values since the impact parameters of the colliding protons in such events will be large.

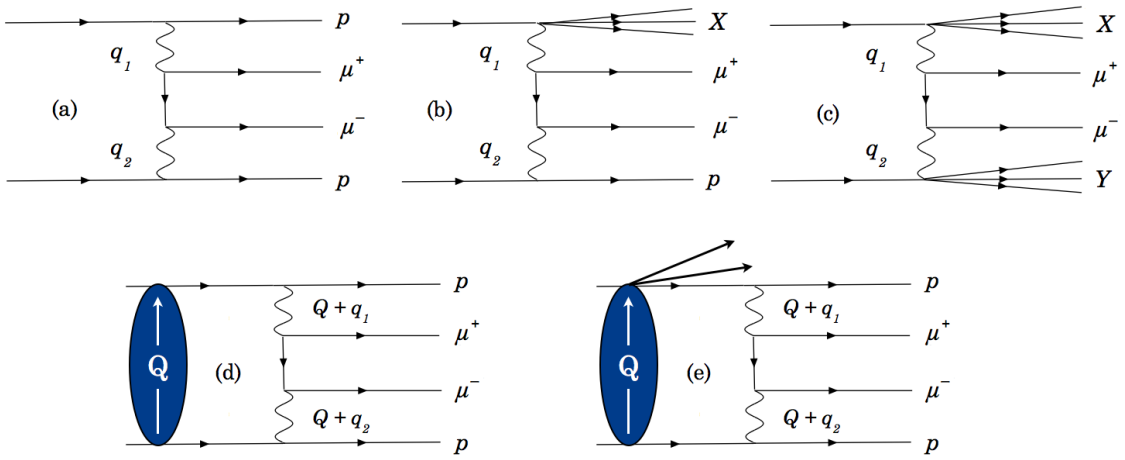

Figure 1 Feyman diagrams showing $\mu^+\mu^-$ production via two-photon fusion. (a) elastic case, (b) semi-inelastic case, (c) fully-inelastic case, (d) elastic case showing a possible rescattering correction where the colliding protons interact via the strong interaction and the energy of the protons is altered, (e) a rescattering correction where the colliding protons interact via the strong interaction and additional particles are produced.

2.2 Inelastic $\mu^+\mu^-$ production via photon fusion

For dimuons produced via photon fusion where one or both of the colliding protons dissociate during the collision process we have for each inelastic vertex a virtual photon flux of the form

$$dn_{inelastic} = dn_{QED}\frac{W_2(q^2,M^2)}{2m_p}dM^2 \approx dn_{QED}\frac{|q^2|}{4\pi^2\alpha}\frac{\sigma_T^{\gamma p}+\sigma_S^{\gamma p}}{M^2-m_p^2}dM^2 \tag{6}$$

Here: $W_2(q^2,M^2)$ is the inelastic scattering structure function, M is the invariant mass of the hadronic system produced in the dissociation, $\sigma_T^{\gamma p}$ and $\sigma_S^{\gamma p}$ are the γp cross-sections for transversely polarised and scalar interactions respectively and α is the fine structure constant. Feyman diagrams for events where one proton dissociates and for events where both protons dissociate, from now on refered to as semi-inelastic and fully-inelastic events respectively, are shown in Figures1(b) and 1(c). Due to uncertainties in the momentum distributions of the quarks within the proton and the collective excitations of these quarks the matrix element describing inelastic vertices is not as well known as the matrix element for elastic vertices. This results in much higher uncertainties in the predicted cross-section for inelastic dimuon production via photon fusion. For the purposes of a luminosity measurement it is therefore not advantageous to include such events. As we show in subsequent sections of this note the inelastic contribution can be suppressed using offline kinematic cuts.

2.3 Rescattering corrections

In addition to the inelastic processes shown in Figures 1(b) and 1(c), which take into account the strong interaction *within* the colliding protons, any strong interactions *between* the colliding protons must also be accounted for. In these so called rescattering processes the strong interaction is not mediated by a point-like object and can be viewed as a Pomeron exhange between the protons. Figures 1(d) and 1(e) show schematic representations of such processes for the elastic case where only the energy of the proton is affected and where additional particles are produced during the interaction respectively. It has been shown by Khoze et. al. [10] that the rescattering correction due to interactions like 1(d) has the effect of modifying the phase of the matrix element but does not change the predicted cross-section for elastic dimuon production via two photon fusion. However, the rescattering correction due to events like those shown in Figure 1(e) has the effect of reducing the rate of $pp \rightarrow p+\mu^+\mu^-+p$ events and increasing the rate of $pp \rightarrow \mu^+\mu^-+X$ events. The calculations of Khoze et. al. [10] have also shown that for a $\mu^+\mu^-$ pair produced with a mass of 20 GeV/c^2 at a rapidity of zero and having a dimuon pair transverse momentum ($P_T^{\mu\mu}$) below 50 MeV/c the appropriate correction to the elastic cross-section is small $\sim 0.13\%$. It was also

shown that, unlike elastic events, such rescattering corrections do not result in a sharp peak at $\phi_{\mu\mu} = 0$ in the dimuon acoplanarity[a] distribution. Therefore by selecting events with $P_T^{\mu\mu} < 50$ MeV/c and small acoplanarity values the contamination due to events where such rescattering occurs can be reduced to a negligible level.

3 Signal events

A Monte Carlo sample of 1×10^5 pp $\rightarrow$ p $+ \mu^+\mu^- +$ p events was used in this analysis. These events were generated with a version of the LPAIR[b] [12] event generator, which performs a full Leading Order (LO) matrix element calculation, and the detector effects were simulated using the detector geometry described by Dbase v22r4 and Gauss v15r21. The detector digitization was performed by Boole v6r5 and event reconstruction by Brunel v24r6. To speed up the generation process each muon in the generated events were required to have

1. Pseudorapidities in the range $1.6 < \eta < 5$
2. A transverse momentum of $P_T > 0.9$ GeV/c
3. A momentum of P > 7.5 GeV/c

Within the fiducial volume, v, defined by these production cuts LPAIR predicts a cross-section of $\sigma_{el}(v) = (88.77 \pm 0.32)$pb. The analysis of these events outlined in this note has been performed using the LHCb analysis package DaVinci v12r14.

3.1 Signal event characteristics

The experimental signature of elastic $\mu^+\mu^-$ pairs produced via two-photon fusion is very distinctive. These events will contain a $\mu^+\mu^-$ pair produced back to back in the transverse plane, thus having small acoplanarity values peaked at zero, and no other particles. In addition the muon pair will have: an invariant mass, $M_{\mu^+\mu^-}$, that will be peaked towards zero and will fall off exponentially for higher mass values, and a pair transverse momentum, $P_T^{\mu\mu}$, that also peaks at low values and falls off exponentially for higher transverse momentum values. The particle multiplicity, dimuon invariant mass, pair transverse momentum and acoplanarity distributions for pp $\rightarrow$ p $+ \mu^+\mu^- +$ p events that pass the L0 and L1 triggers and are then reconstructed are shown in Figure 2.

3.2 Geometric acceptance

We define the geometric acceptance, A_{el}^{geom}, to be the fraction of events satisfying the generator level production cuts (1-3) that contain two muons that are reconstructible at Monte-Carlo truth level. Using a sample of 1×10^5 fully simulated pp $\rightarrow$ p $+ \mu^+\mu^- +$ p events and the DaVinci analysis package we have determined A_{el}^{geom} to be 0.9207 ± 0.0009(stat.).

3.3 Efficiencies

The reconstruction efficiency, ε_{el}^{reco}, and trigger efficiency, $\varepsilon_{el}^{trigger}$, will be determined from data once it arrives (see Sections 7.5 and 7.6). However, we now present estimates of these efficiencies that were obtained using the full LHCb detector simulation. We also outline a proposed new dimuon stream at the L0 trigger level that has been used in this analysis that will allow pp $\rightarrow$ p $+ \mu^+\mu^- +$ p events to be recorded at LHCb.

[a]Here we define the dimuon acoplanarity by $\phi_{\mu\mu} = \pi - cos^{-1}((P_x^+ P_x^- + p_y^+ P_y^-)/(P_T^+ P_T^-))$ where the superscripts, + and -, refer to the μ^+ and μ^- respectively. Since the acoplanarity is $\pi-$ the difference in azimuthal angle between the two muons, events with $\phi_{\mu\mu}$= 0 correspond to those which are back-to-back in the transverse plane.

[b]We are most grateful to Andrey Shamov and Valery Telnov for providing us with a copy of their modified version of the LPAIR generator.

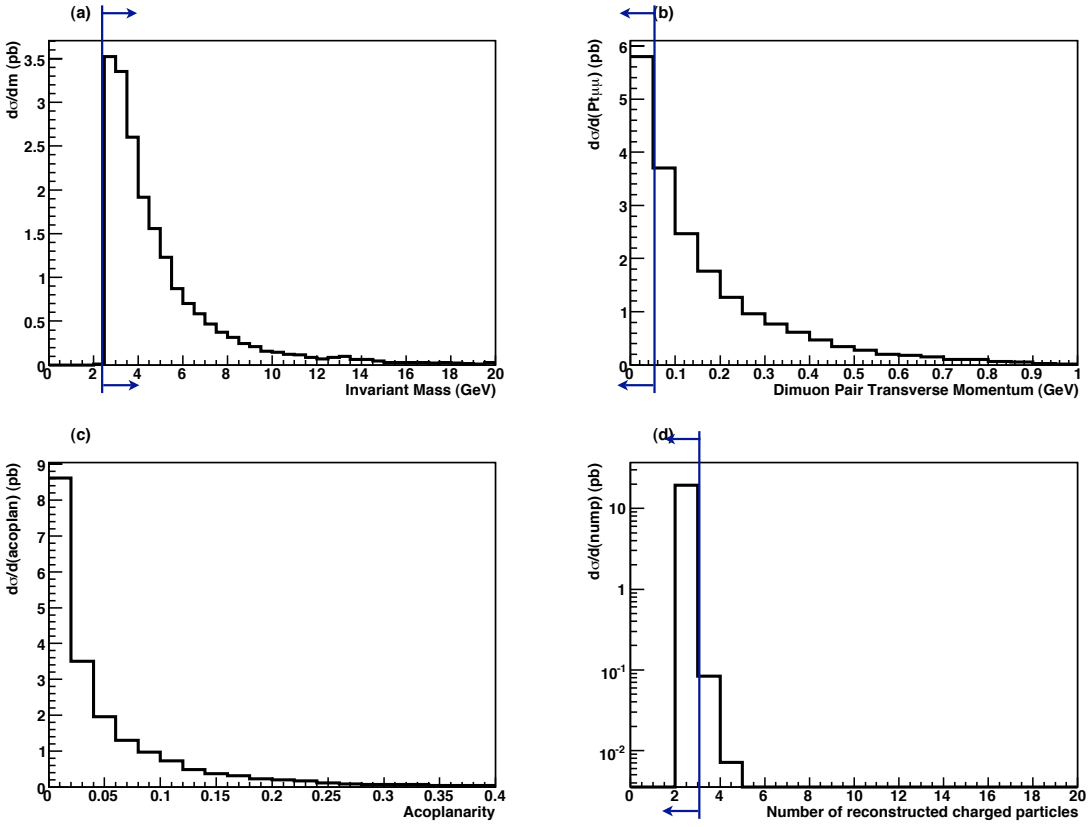

Figure 2 Event characteristics of fully simulated and triggered events containing dimuon pairs produced via elastic two-photon fusion. (a) Dimuon invariant mass. (b) Dimuon pair transverse momentum. (c) Dimuon acoplanarity. (d) Event particle multiplicity. The offline kinematic cuts described in Section 5 are highlighted.

3.3.1 Reconstruction efficiency

The reconstruction efficiency, ε_{el}^{reco}, is defined to be the fraction of events within the LHCb geometric acceptance that can be reconstructed offline. It can be expressed as the product of three components:

$$\varepsilon_{el}^{reco} = (\varepsilon_{trk}^{(1)} \times \varepsilon_{match}^{(1)} \times \varepsilon_{id}^{(1)}) \times (\varepsilon_{trk}^{(2)} \times \varepsilon_{match}^{(2)} \times \varepsilon_{id}^{(2)}) \tag{7}$$

Here ε_{trk} is the efficiency of reconstructing the track of one of the muons coming from the elastic two-photon fusion process. ε_{match} accounts for the efficiency of reconstructing a muon tower in the muon chambers and matching it to this track. Finally, for tracks that have been matched to muon towers, ε_{id} is the efficiency of any additional muon identification criteria, e.g. calorimeter energy requirements, that will be used to increase the purity of the muon samples. The superscripts refer to muon 1 and muon 2. Possible methods for determining ε_{trk}, ε_{match} and ε_{id} from data and the expected associated measurement uncertainties are discussed in Section 7. From simulation ε_{el}^{reco} has been determined to be 0.5351 ± 0.0016(stat.).

3.3.2 Proposed modification to the L0 trigger

In its current implementation (up to and including DaVinci v19r8) for an event to pass the L0 dimuon trigger level it is required that

1. The sum of transverse momenta of all the muons in the event, $\sum P_T^{\mu}$, must be greater than or equal to 1.5 GeV/c.
2. A total global transverse energy, E_T, from the electromagnetic and hadronic calorimeters of 5 GeV or more.

It should be noted that the first condition makes no requirement on the number of muons reconstructed by the L0 trigger system and an event containing only one muon with $P_T > 1.5$ GeV/c can be passed by this stream. The second requirement is designed to guard against muons from the beam halo consuming a large amount of the bandwidth. Since $pp \to p + \mu^+\mu^- + p$ events only contain two muons and no other particles they will only rarely result in an E_T satisfying the second requirement and thus practically none of our signal events pass the L0 trigger. Consequently we propose to introduce a new dimuon line at the L0 level that will allow $pp \to p + \mu^+\mu^- + p$ events to pass while at the same time keeping the bandwidth consumed by halo muons to a low level. The new stream has the following two requirements

1. The sum of transverse momenta of all the muons in the event, $\sum P_T^{\mu}$, must be greater than or equal to 1.5 GeV/c.
2. The L0 trigger system must reconstruct more than one muon.

Preliminary investigations of this new dimuon trigger stream suggest that it will allow beam halo events to pass at a rate of ~ 200 Hz which constitutes 0.02% of the total L0 bandwidth [13].

3.3.3 Trigger efficiencies

Due to the current development of the Higher Level Trigger (HLT) we have not included it in our efficiency studies but have instead used the old L1 trigger level as a substitute. The HLT will be investigated for the $pp \to p + \mu^+\mu^- + p$ channel in the future before data taking begins.We define the total trigger efficiency from the combination of the conditional probabilities that an event passes each trigger stage.

$$\varepsilon_{el}^{trigger} = \varepsilon_{el}^{L0} \times \varepsilon_{el}^{L1} \tag{8}$$

Here ε_{el}^{L0} is the fraction of events that can be reconstructed offline that would pass the L0 trigger algorithm which includes the new dimuon stream outlined in the previous section, ε_{el}^{L1} is the fraction of events that can be reconstructed offline and pass the L0 trigger that also pass the L1 trigger algorithm. Table 1 summarises

the acceptances and efficiencies for $pp \to p + \mu^+\mu^- + p$ events at LHCb. The calculation of the acceptance due to our offline kinematic selection criteria, A_{el}^{kin}, is discussed in Section 5.

Stage	Symbol	Efficiency
Detector acceptance	A_{el}^{geom}	0.9207 ± 0.0009
Reconstruction	ε_{el}^{reco}	0.5351 ± 0.0016
L0 algorithm	ε_{el}^{L0}	0.6190 ± 0.0022
L1 algorithm	ε_{el}^{L1}	0.7135 ± 0.0026
Kinematic acceptance	A_{el}^{kin}	0.2697 ± 0.0030
Total efficiency (forward measurement)	ε_{el}^{total}	0.0587 ± 0.0008

Table 1 Acceptance, reconstruction and trigger efficiencies for $pp \to p + \mu^+\mu^- + p$ events at LHCb. Statistical errors are shown.

4 Background processes

The strongest backgrounds to our signal are events containing dimuon pairs produced via inelastic two-photon fusion and double pomeron exchange. We have studied these processes by interfacing the LPAIR and DPEMC [14] Monte-Carlo generators to the full LHCb detector simulation. In addition we have considered a number of other Standard Model processes such as $b \to \mu^- + Y$, $\bar{b} \to \mu^+ + X$ and events where two hadrons are both mis-identified as muons. These backgrounds have been investigated at four vector level by examining large Monte-Carlo samples generated using the PYTHIA and DPEMC generators. The background samples that have been studied are summarised in Table 2 and are described in the following sections.

Background process	$\sigma \times BR$ (pb)	Events generated	$\int \mathcal{L}dt$ equivalent
multicolumn4lStudied with full LHCb simulation			
$pp \to p + \mu^+\mu^- + X$ ($\gamma\gamma$)	42.52	2.5×10^4	588 pb^{-1}
$pp \to Y + \mu^+\mu^- + X$ ($\gamma\gamma$)	28.01	1×10^4	357 pb^{-1}
$pp \to Y + \mu^+\mu^- + X$ (DPE)	120	2.5×10^4	207 pb^{-1}
Studied at 4 vector level			
$b \to \mu^- + Y$, $\bar{b} \to \mu^+ + X$	5×10^6	5×10^7	10 pb^{-1}
$c \to \mu^- + Y$, $\bar{c} \to \mu^+ + X$	3.5×10^7	3.5×10^8	10 pb^{-1}
$\gamma^*/Z \to \mu^+\mu^-$	2×10^4	1×10^7	500 pb^{-1}
$J/\psi \to \mu^+\mu^-$	4.63×10^6	4.63×10^7	10 pb^{-1}

Table 2 Standard Model background samples that have been used in this analysis. The two-photon fusion ($\gamma\gamma$) and double Pomeron exchange (DPE) samples were produced with the LHCb detector simulation software chain (Gauss, Boole and Brunel) and the LPAIR and DPEMC Monte-Carlo event generators respectively. The samples that have been studied at 4 vector level were produced using the PYTHIA Monte-Carlo generator

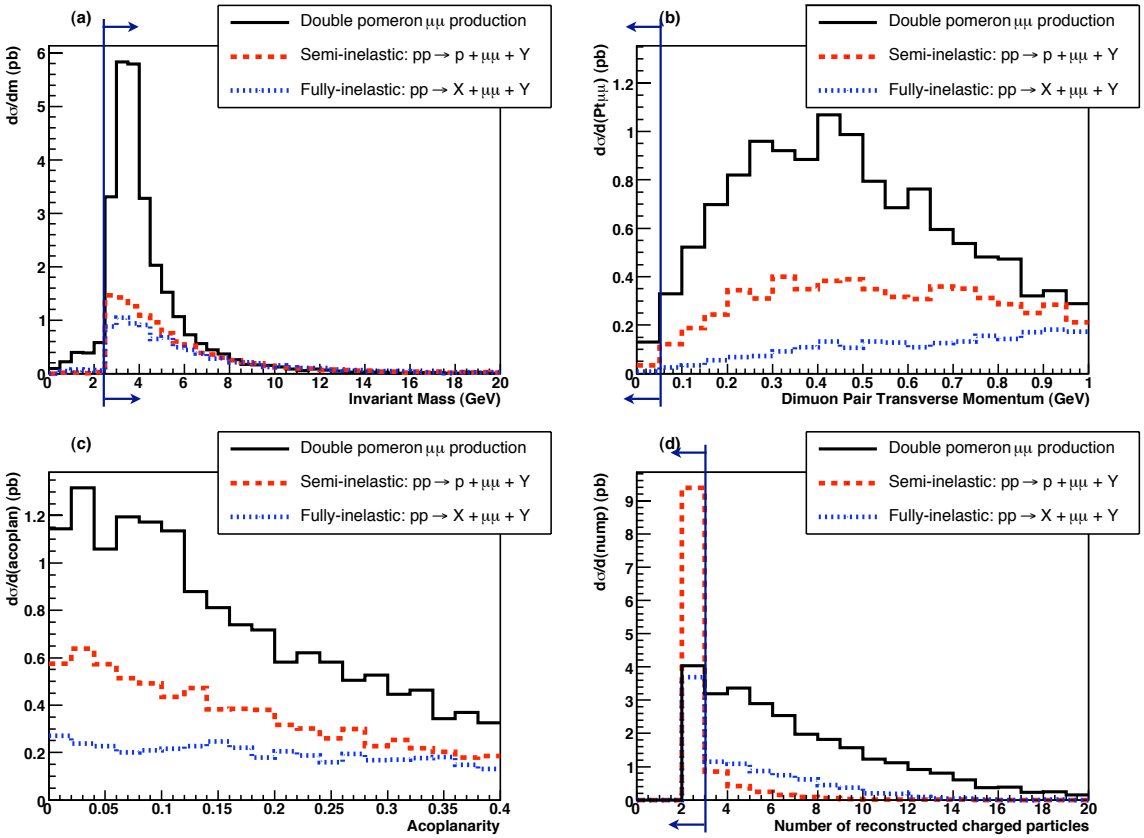

Figure 3 Fully simulated and triggered events that contain a $\mu^+\mu^-$ pair produced via double Pomeron exchange or inelastic two photon fusion. (a) Dimuon invariant mass. (b) Dimuon pair transverse momentum. (c) Dimuon acoplanarity. (d) Event particle multiplicity. The offline kinematic cuts described in Section 5 are highlighted.

4.1 Dimuon pairs produced via inelastic two-photon fusion

Monte-Carlo samples of 2.5×10^4 and 1×10^4 events have been generated and analysed for the semi-inelastic and fully-inelastic two-photon fusion processes respectively. These events were produced with the LPAIR generator using the soft proton structure functions of A.Suri and D. Yennie [15]. The LHCb detector effects were simulated using the detector geometry described by Dbase v22r4 and Gauss v15r21. The detector digitization was performed by Boole v6r5 and event reconstruction by Brunel v24r6. To speed up the generation process both muons in the generated events were required to satisfy the production cuts (1 - 3) described in Section 3.

Figure 3 shows the dimuon invariant mass, pair transverse momentum, acoplanarity and particle multiplicity distributions for events within these samples that are fully reconstructed and that pass the L0 and L1 trigger levels. By comparing these four distributions with the corresponding elastic distributions shown in Figure 2 it can be seen that for dimuons produced via inelastic two-photon fusion: the invariant mass distributions are very similar to the distribution for elastic events; the acoplanarity distributions are relatively flat compared to the corresponding distributions for the elastic events; the dimuon pair pair transverse momentum distributions peak at higher values ($\sim$600 MeV/c for semi-inelastic events and 1100 MeV/c for fully-inelastic events) than for elastic events; the particle multiplicity distributions have larger tails than our signal events.

4.2 Dimuon pairs produced via double Pomeron exchange

A sample of 2.5×10^4 dimuon events produced via double Pomeron exchange have been examined. These events were generated with the DPEMC event generator. Within DPEMC these dimuons are produced via

the Drell-Yan process within the Pomeron-Pomeron collision. Since DPEMC applies a cut of $q^2 > 1$ GeV/c to the initial state parton showers of such processes and the events that we are interested in typically have values less than this only the P_T of the Pomeron system and not the P_T of the colliding quarks relative to the parent Pomerons will contribute to the dimuon pair P_T[c]. To correct for this we have applied a gaussian addition of 350 MeV/c to the P_T of the partons partaking in the initial state shower, a value that is consistent with previous theoretical studies [16]. The effects of the LHCb detector have been simulated using the geometry described by Dbase v22r4 and Gauss v15r21. The detector digitization was performed by Boole v6r5 and event reconstruction by Brunel v24r6. To speed up the generation process only events containing a dimuon pair with individual pseudorapidities in the range $1.7 < \eta < 5.1$ and a mass above 2 GeV/c^2 have been generated.

The cross-section for these events at the LHC has been calculated using two different theoretical models, the inclusive double Pomeron exchange model of Boonekamp, Peschanski and Royon (BPR) [17] and the factorized model of Cox and Forshaw [18]. In addition, the uncertainty due to our knowledge of the Pomeron parton distribution functions has been estimated using different sets of Pomeron PDFs based on data collected at the Hera e-p collider. The BPR predictions have been recalculated using NLO fits to Zeus and H1 data collected between 1997-2000 and a fit to the combined data-set from both experiments [19] (labeled respectively ZEUSnl, H1nl and ZEUS+H1nl in Table 3). The CF model has been recalculated using H1nl as well as two fits to data collected by H1 in 2006 (H106FitA and H106FitB) [20]. Table 3 summarises predictions of the BPR and CF models using the different Pomeron PDF sets. With the exception of the ZEUSnl PDF set, there is a reasonable agreement between the models. We have taken the cross-section to be 120 pb and have assigned an uncertainty due to the theoretical modelling and knowledge of the Pomeron flux and PDFs to be $\pm$ 60 pb.

	ZEUSnl	H1nl	ZEUS+H1nl	H106FitA	H106FitB
BPR	571	73	85		
CF		110		167	178

Table 3 Cross-section predictions, in picobarns, for dimuon events produced via double Pomeron exchange due to the Boonekamp, Peschanski and Royon (BPR) and Cox-Forshaw (CF) models using the six different Pomeron PDF sets described in the text.

The dimuon mass, pair tranverse momentum, acoplanarity and particle multiplicity distributions for events within this sample that pass the L0 and L1 trigger levels and are then reconstructed are shown in Figure 3. With the exception of the particle multiplicity distribution, which is flatter and extends up to high values, the distributions for these events have shapes that are similar to those for dimuons produced via semi-inelastic two photon fusion.

4.3 Other Standard Model backgrounds

In addition to these backgrounds we have also examined the contamination due to four other Standard Model processes: dimuons produced via the Drell-Yan process $\gamma^*/Z \to \mu^+\mu^-$, $b\bar{b}$ events where both b quarks decay semi-leptonically to muons $b \to \mu^- + Y$, $\bar{b} \to \mu^+ + X$, $c\bar{c}$ events where both c quarks decay semi-leptonically to muons $c \to \mu^- + Y$, $\bar{c} \to \mu^+ + X$ and dimuons produced via the decay of J/ψ particles. These processes have been studied at four vector level using event samples generated using the PYTHIA event generator. For each of these background samples any event that contains at least two oppositely charged muons with pseudorapidity values in the range, $1.9 < \eta < 4.9$ and having $P_T > 1$ GeV/c and $P > 8$ GeV/c has been examined as a potential background event. Aside from these criteria we have conservatively assumed reconstruction and trigger efficiencies for these samples of 100%. The particle multiplicity for these four vector events has been estimated by counting the number of stable charged particles with momenta above 500 GeV/c that have pseudorapidity values lying within $1.9 < \eta < 4.9$. The sizes of the samples used are summarised in Table 2 while the particle multiplicity, dimuon acoplanarity, invariant mass and pair transverse momentum distributions for these processes are shown in Figure 4.

Unlike our signal process the dimuon acoplanarity distributions are relatively flat and fall off less dramatically for higher values. The dimuon pair transverse momentum distributions for these processes peak at

[c] We are most grateful to Andrey Shamov for bringing this point to our attention.

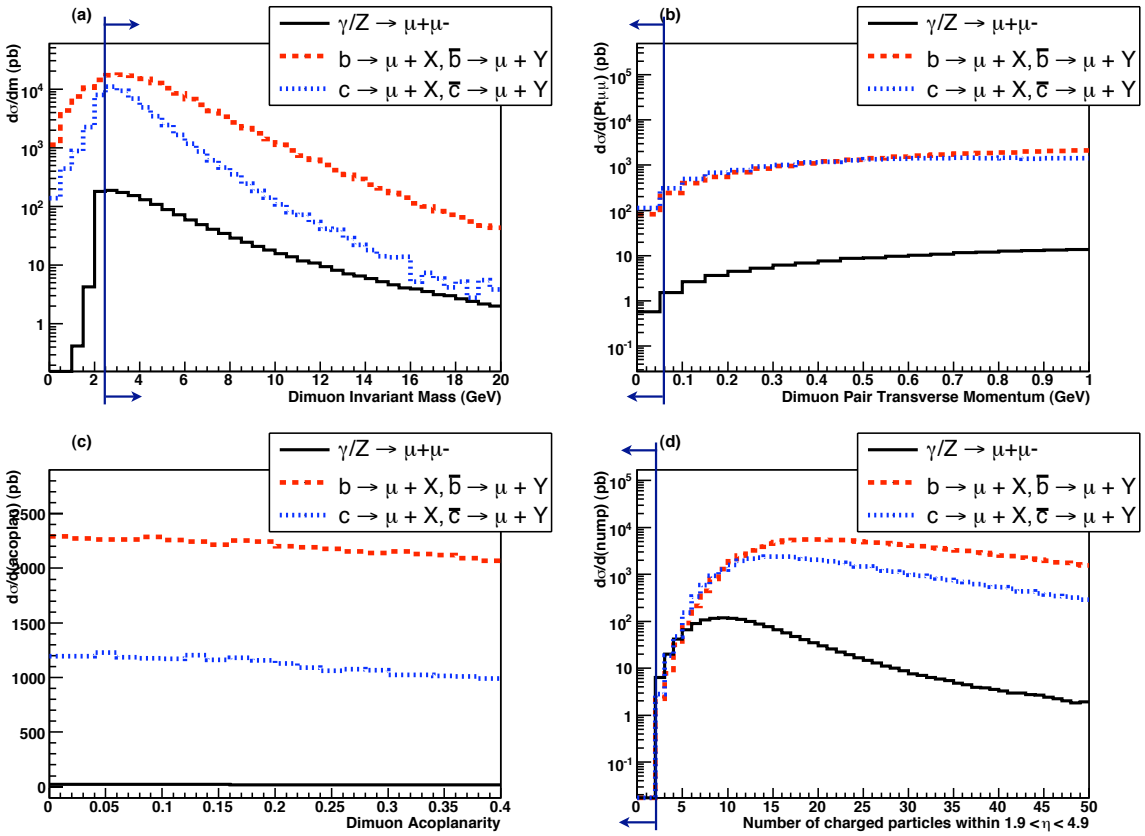

Figure 4 Monte-Carlo level events containing a dimuon pair produced via a number of Standard Model processes, here we have assumed a reconstruction and trigger efficiency of 100%. (a) Dimuon invariant mass. (b) Dimuon pair transverse momentum. (c) Dimuon acoplanarity. (d) Event particle multiplicity. The offline kinematic cuts described in Section 5 are highlighted.

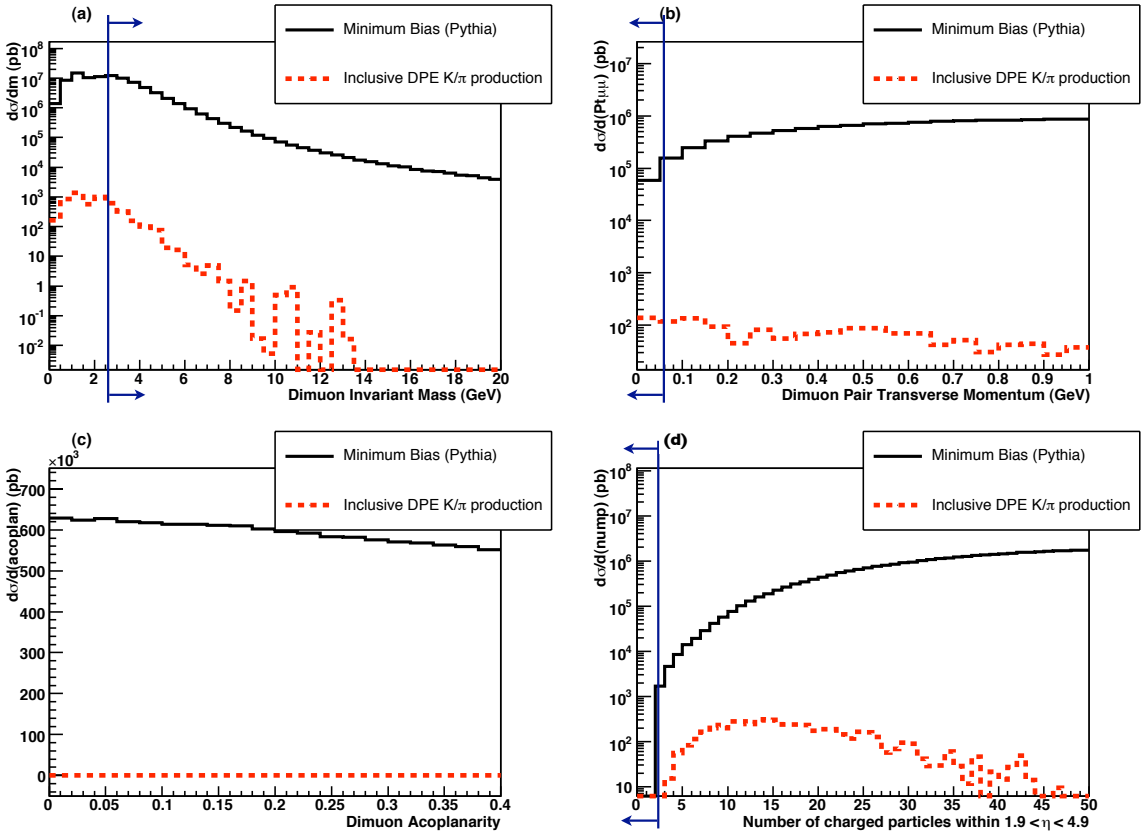

Figure 5 Parameter distributions for combinations of opposite charge kaons and pions coming from minimum-bias and double Pomeron exchange events. Here the distributions have been scaled according to the hadron mis-id probabilities discussed in the text and we have assumed a reconstruction and trigger efficiency of 100%. (a) Dimuon invariant mass. (b) Dimuon pair transverse momentum. (c) Dimuon acoplanarity. (d) Event particle multiplicity. The offline kinematic cuts described in Section 5 are highlighted.

much higher values (> 1.4 GeV/c) than our signal and combinded have an effective cross-section of ∼200 pb for values below 50 MeV/c^2. The particle multiplicity distributions peak between 10 and 25 and fall off to ∼4 pb for events containing less than three charged particles within the LHCb acceptance while the dimuon invariant mass distributions peak at low mass values and, with the exception of the Drell-Yan distribution which peaks again at the Z pole (∼91 GeV/c^2), fall off exponentially for higher masses.

4.4 Hadron mis-identification

The last important source of background events comes from random combinations of oppositely charged pions or kaons that are both mis-identified as muons. We have estimated the magnitude of this background contribution in the following manner. Firstly, having assumed that there are two principle ways in which mis-identification can occur decay in flight and "punchthrough", we have estimated the probability of mis-id as a function of hadron momentum (for details on how this was achieved see [7]). These mis-id probabilities were then combined with the expected rate of random K/π combinations from a variety of sources. Most of these sources have been studied using a sample of ten million minimum bias[d] events generated using PYTHIA. In addition we have attempted to quantify the level of contamination due to di-hadron production via double Pomeron exchange since the characteristics of these events may be similar to those of our signal process. We have done this by examining two event samples generated with the DPEMC generator. One sample containing two million events where a di-jet is produced inclusively via double Pomeron exchange and one containing one million events where two gluons are produced exclusively via double Pomeron exchange. Using these two DPE samples and the minimum-bias sample and only considering pions and kaons with pseudorapidity values in the range $1.9 < \eta < 4.9$ and momenta satisfying

[d]Corresponding to the PYTHIA process (ISUB) flags 11, 12, 13, 28, 53, 68, 86, 87, 88, 89, 91, 92, 93 ,94, 95, 106, 107 and 108.

P > 8 GeV/c and P_T > 1 GeV/c, all the opposite charge pairwise hadron combinations (i.e. $\pi^+\pi^-$, $K^+\pi^-$, $K^-\pi^+$ and K^+K^-) in these events were recorded. The probability of mis-identification for each hadron was calculated and an overall weighting assigned to each dihadron combination based on these probabilities. Aside from these criteria we have assumed reconstruction and trigger efficiencies for these samples of 100%. The particle multiplicity for these four vector events has been estimated by counting the number of stable charged particles with momenta above 500 GeV/c that have pseudorapidity values lying within 1.9 < η < 4.9. The various distributions for these dihadron combinations are shown in Figure 5.

5 Signal selection and background reduction

Given the particle multiplicity, dimuon invariant mass, pair transverse momentum and acoplanarity distributions of our signal events as shown in Figure 2, and the corresponding background distributions as shown in Figures 3, 4 and 5, the following kinematic cuts are proposed:

1. The dimuon pair transverse momentum must satisfy $P_T^{\mu\mu}$ < 50 MeV/c.
2. There must be less than 3 reconstructed charged particles in the event.
3. The dimuon invariant mass must be in the range 2.6 GeV/c^2 < $M_{\mu\mu}$ < 20 GeV/c^2.
4. The mass region 3 - 3.2 GeV/c^2 is excluded.

Criteria 1, in addition to its effectiveness at reducing the backgrounds described in Section 4, has the effect of reducing the uncertainty on the predicted signal cross-section, due to rescattering corrections and uncertainties in the electromagnetic form factors of the proton, to < 1%. The invariant mass cuts 3 and 4 are designed to further reduce the background contribution coming from the decays $Z \to \mu^+\mu^-$ and $J/\psi \to \mu^+\mu^-$ respectively. The effects of these selection criteria are discussed in the next two sections.

5.1 Kinematic Acceptance

The acceptance of these offline kinematic cuts, A_{el}^{kin}, is defined to be the fraction of offline reconstructed $pp \to p + \mu^+\mu^- + p$ events passing all of the the trigger stages that also satisfy these kinematic requirements. Using the full detector simulation A_{el}^{kin} was determined to be 0.2697 $\pm$ 0.003. Combining this with the geometric acceptance and the reconstruction and trigger efficiencies given in Section 3 yields an overall efficiency of 0.0587 $\pm$ 0.0008(stat.). This gives an effective signal cross-section of $\sim$5.21 pb which corresponds to 5210 $\pm$ 71(stat.) events in half a nominal year of LHCb running (1 fb^{-1} of data).

5.2 Background estimation

The expected background composition after the selection cuts have been applied is summarised in Table 4. Applying the cuts to the background samples described in Section 4 reduces the background to a level that is (4.1 $\pm$ 0.5(stat.))% of the expected signal rate. This equates to $\sim$214 background events per 1 fb^{-1}. The background is dominated by events caused by K/π mis-identification at a rate of $\sim$121 events per 1 fb^{-1}. In principle it should be possible to accurately assess the level of pion/kaon background from data once it arrives. Events containing dimuon pairs produced by double Pomeron exchange or inelastic two photon fusion contribute to the overall background roughly equally (each contributing $\sim$1% of the signal level).

It should be noted that due to the limited size of the Drell-Yan, heavy quark and pion/kaon mis-id samples the effect of cuts 2 - 4 and cut 1 have been evaluated separately. The effect of cut 1 on events that have already passed cuts 2 - 4 was estimated by calculating the probability that an event will satisfy $P_T^{\mu\mu}$ < 50 MeV/c as a function of the events' particle multiplicity. Figure 6 shows this probability for the four samples. The dependence of this probability on the event multiplicity was parameterised by fitting straight lines was to the four distributions. Using these parameterisations the probability that $P_T^{\mu\mu}$ < 50 MeV/c when the particle multiplicity is less than three was calculated for each background sample. An overall background

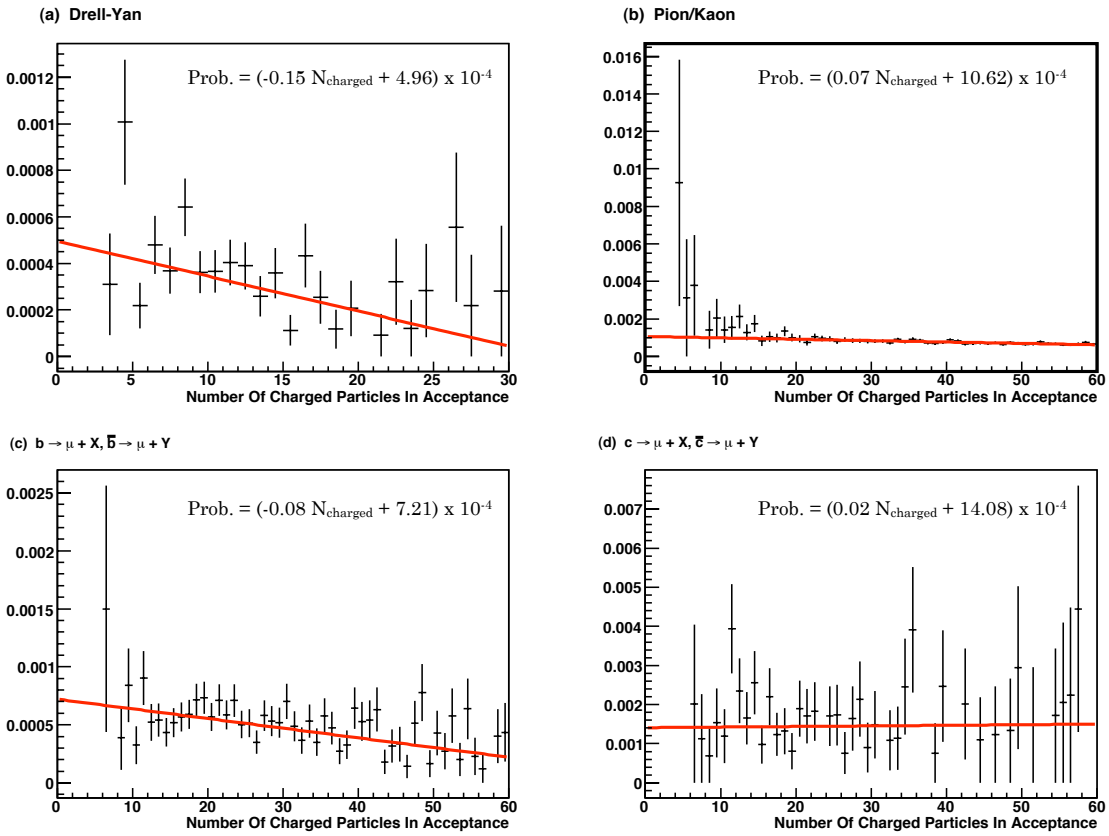

Figure 6 Probability of dimuon pair transverse momentum being less than 50 MeV/c for events within the invariant mass range defined by cuts 1-2 as a function of the number of charged particles within the LHCb acceptance. (a) $\gamma^*/Z \to \mu^+\mu^-$. (b) Random pion/kaon combinations. (c) $b\bar{b}$ events where both b quarks decay semi-leptonically to muons. (d) $c\bar{c}$ events where both c quarks decay semi-leptonically to muons. The line is the best straight-line fit to the data points.

Process	Events per fb^{-1}	Statistical uncertainty	Systematic uncertainty
$\text{pp} \to \text{p} + \mu^+\mu^- + \text{p}$ (signal)	5210	± 71	± 17
Inclusive DPE $\mu^+\mu^-$ production	52	± 15	± 26
$\text{pp} \to \text{p} + \mu^+\mu^- + \text{X}$	31	± 7	± 10
$\text{pp} \to \text{Y} + \mu^+\mu^- + \text{X}$	8	± 5	± 4
$\text{b}\bar{\text{b}} \to \mu^+ + \mu^- + \text{X}$	1	± 0.5	± 1
$\text{c}\bar{\text{c}} \to \mu^+ + \mu^- + \text{X}$	2	± 1	± 2
$\text{J}/\psi \to \mu^+\mu^-$	0	$+1$	$+1$
$\gamma^*/\text{Z} \to \mu^+\mu^-$	2	± 0.3	± 2
K/π mis-identification	121	± 19	± 12 (from data)
Total Background	217	± 26	± 30

Table 4 The expected number of events for the signal and background sources per fb^{-1} of data after the selection cuts outlined in Section 5 have been applied. Statistical uncertainties due to our sample sizes and systematic uncertainties due to the errors on the predicted cross-sections are shown (see Section 6 for more details).

estimate was made by combining this probability with the calculated probability that the events pass cuts 2 - 4. The uncertainties on the straight line fits were included in the overall uncertainties of our background estimates.

The mass window proposed in cut 4 is designed to remove the contamination due to the process $\text{J}/\psi \to \mu^+\mu^-$. Since the reconstructed width of the J/ψ mass at LHCb via the dimuon channel is $\sim$10 MeV/c^2 [21] we have chosen a window of $\pm$100 MeV/c^2 and expect a corresponding $\text{J}/\psi \to \mu^+\mu^-$ supression of $\sim 10^{-12}$ which equates to much less than 1 event per fb^{-1} of data.

6 Pile-up correction

The proposed kinematic selection requires that there are less than three reconstructed charged particles in a given event in order for it to be accepted. This is problematic since at the LHC there will be a non-zero probability that a given bunch crossing will result in more than one proton-proton interaction. Assuming an LHCb running luminosity of 2×10^{32} $\text{cm}^{-2}\text{s}^{-1}$ and an LHC inelastic cross-section of 80 mb the probabilities that a bunch crossing will result in 0, 1, or more than 1 interaction are respectively: $P_0 = 0.57$, $P_1 = 0.31$, and $P_{>1} = 0.12$. Since these probabilities are dependent on the inelastic cross-section, which is not known accurately from theory, they must be measured using data. A possible method for making such a measurement at LHCb using the pile-up detector has been investigated previously by N. Zaitsev [22]. The pile-up detector is located upstream of the Vertex Locator and consists of a set of two planes of silicon strip detectors equipped with fast readout electronics to allow their data to be made available at the L0 trigger level. During a given running period the number of bunch crossings containing i proton-proton interactions, N_i^m, can be counted. The number counted in this way can then be related to the actual number, N_i, if the efficiency for detection, ε_i, is known. Since we will only select single interaction dimuon events produced via elastic two photon fusion, N_1^{el}, we will need to relate this number to the total number of signal events from bunch crossings of all types, N^{el}, which is equal to

$$N^{el} = N_1^{el} + N_{>1}^{el} = N_1^{el}(1+f) \tag{9}$$

Here $N^{el}_{>1}$ is the number of signal events produced in bunch crossings that contain more than one proton-proton interaction and f is the correction that must be determined from data and will be given by

$$f = \frac{N^{el}_{>1}}{N^{el}_{1}} \simeq \frac{N^{m}_{>1}\varepsilon_1 - N^{m}_{1}(1-\varepsilon_1)}{N^{m}_{1}\varepsilon_{>1} - N^{m}_{>1}(1-\varepsilon_{>1})} \tag{10}$$

Since the statistical uncertainties on N^{m}_{1} and $N^{m}_{>1}$ will be <0.1% in as little as one second of data the dominant uncertainty on a measurement of f will be due to the uncertainties on the determination of the efficiencies ε_1 and $\varepsilon_{>1}$. These efficiencies can be determined readily using Monte-Carlo studies, however, a measurement using real data would be preferable and it is envisioned that a viable method for achieving this will be developed before data-taking begins.

An alternative method for determining the pile-up correction can be performed offline using random triggers and the full Velo reconstruction. Counting the number of primary vertices in a randomly triggered event will allow the relative number of bunch crossings that result in 0,1 or more than one interaction.

7 Systematic and statistical uncertainties

From equation 1 it can be seen that the accuracy with which an integrated luminosity measurement can be made using the rate of dimuons produced via elastic photon fusion will be limited by the statistical and systematic uncertainties on: the number of $pp \rightarrow p + \mu^+\mu^- + p$ candidates observed; the expected number of background events; the geometric and kinematic acceptances; the trigger and reconstruction efficiencies; the predicted cross-section of $pp \rightarrow p + \mu^+\mu^- + p$ events at LHCb. We will discuss the uncertainties from each of these sources in turn. The estimated systematic uncertainties from each source are summarised in Table 5.

7.1 Predicted cross-section

As outlined in Section 2 the uncertainty on the predicted cross-section of our signal process, σ_{el}, will have two components, one from the rescattering corrections due to strong interactions between the colliding protons and the other due to the accuracy of measurements of the proton electromagnetic form factors G_M and G_E.

Rescattering corrections: The events that pass our offline selection criteria will have dimuon pair transverse momenta of less than 50 MeV/c. It has been shown by Khoze et. al. [10] that for dimuon pairs produced via two photon fusion with a mass of 20 GeV/c^2, a rapidity of zero and a pair transverse momentum below 50 MeV/c the appropriate correction to σ_{el} is $\sim$0.13%. This value has been taken as the systematic uncertainty from this source, however, further studies may be required since the events that will be reconstructed at LHCb will have lower masses and higher rapidities than those described in [10].

Electromagnetic form factors: As outlined in Section 2 our elastic dimuon event sample will have two components: events where the impact parameters of the colliding protons are large (which allows the protons to be treated as point-like objects) and the process is only sensitive to the proton mass, charge and anomalous magnetic moment (which have been measured with an uncertainty below 0.001%) and events where the protons impact parameters are small and the process is sensitive to the electromagnetic form factors of the proton (which have been measured with an uncertainty of $\sim$2%). If the predicted elastic cross-section is to have an associated uncertainty below 1% the event rate of elastic processes that are sensitive to the electromagnetic form factors must be below 50% of the point-like event rate. This can be achieved by selecting events that have small dimuon pair transverse momenta ($P^{\mu\mu}_T$) values since the impact parameters of the colliding protons in such events will be large. The offline selection requirement that $P^{\mu\mu}_T$ < 50 MeV/c will reduce the contribution from events sensitive to the electromagnetic form factors to $\sim$15% of the overall event rate. We thus assign a systematic uncertainty of 0.3% to the luminosity measurement due to the measurement precision of G_E and G_M.

7.2 Signal candidates

The uncertainty on the number of $pp \rightarrow p + \mu^+\mu^- + p$ candidates observed, N^{obs}_{el}, will be purely statistical. Using the efficiency and acceptance values we have obtained from simulation, a 1% uncertainty on N^{obs}_{el} will require 10,000 events which equates to $\simeq$2 fb^{-1} of data.

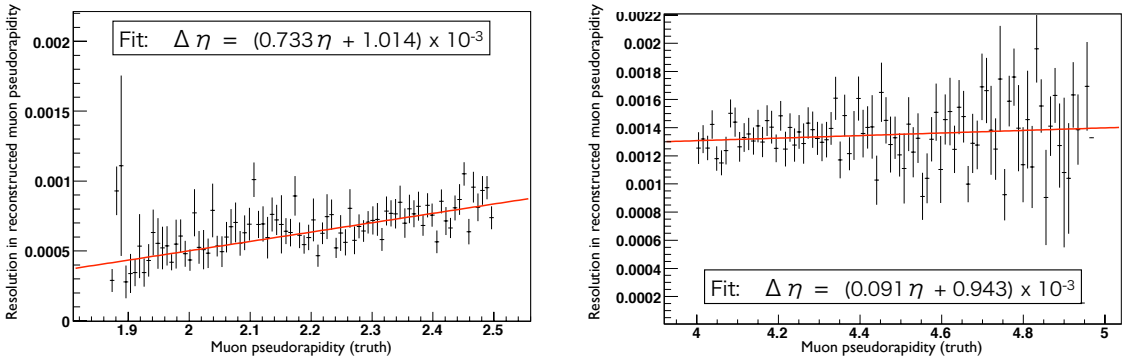

(a) (b)

Figure 7 Reconstructed pseudorapidity resolution as a function of true pseudorapidity for muons reconstructed near the edges of the LHCb detector. (a) low pseudorapidity values corresponding to the outer edge of the detector and (b) high pseudorapidity values corresponding to the detector edge near the beam pipe. The red lines are straight line fits to the data and the fit values are shown.

7.3 Expected number of background events

The main contributions to the expected number of background events, N_{el}^{back}, will come from events where dimuons are produced via either double Pomeron exchange or inelastic two photon fusion and events due to pion/kaon mis-identification. We will discuss each source separately.

Pions/kaons mis-id: It will be possible to measure the background due to pion and kaon mis-identification from data. This can be achieved by measuring the muon mis-identification rate of a pure sample of pions or kaons. For example for pions this can be achieved by examining the pions coming from the decays $K_s \rightarrow \pi^+\pi^-$ and $\Lambda \rightarrow p\pi^-$. Combining these mis-identification probabilities with the measured rate of events containing a di-hadron combination with an invariant mass in the range 2.6 GeV/c^2 < M_{hh} < 20 GeV/c^2 will enable the background to be evaluated. Assuming the mis-id rates for pions and kaons can be determined with an uncertainty of 10% we estimate that the systematic uncertainty on such a measurement will be $\pm$12 events per fb^{-1} of data.

Double Pomeron Exchange: The expected background contribution due to dimuons produced via double Pomeron exchange given in Table 2 assumes a cross-section for this process of 120 pb within the fiducial volume as described in Section 4.2. By comparing cross-section predictions obtained using the BPR and CF DPE models and different Pomeron PDF sets (see Table 3) we estimate the uncertainty on this cross-section prediction, due to uncertainties in our knowledge of the Pomeron fluxes and PDFs and inaccuracies in the theoretical modeling of DPE processes, to be $\pm$ 60 pb. Given this uncertainty and the calculated efficiencies for this process we assign a systematic uncertainty on the number of expected dimuon DPE events of $\pm$ 26 events per fb^{-1} of data.

Inelastic 2-Photon fusion: The uncertainty on the predicted cross-section for the semi and fully inelastic events has been estimated using LPAIR by calculating the effective cross-section for these events within the LHCb acceptance for two different proton structure functions. One set of structure functions is due to Suri and Yennie [15] while the second combines the Suri-Yennie q^2 dependence for the non-resonant contribution with experimental measurements of the the q^2 dependence for the resonance contributions and the photo-production cross-section for $q^2 \rightarrow 0$. We have taken the percentage difference between these two predictions to be the systematic uncertainty on the predicted cross-sections. This results in an effective cross-section for dimuon production via semi and fully inelastic 2-photon fusion events that are triggered, reconstructed and selected offline at LHCb of (31 $\pm$ 10)fb and (8 $\pm$ 4)fb respectively.

7.4 Acceptances

Geometric acceptance: We expect the uncertainty on our geometric acceptance estimate to be dominated by uncertainties due to the tracking resolution near the edges of the LHCb detector. Using the muon tracks from our signal process that have been passed through the LHCb detector simulation the resolution in

the reconstructed muon pseudorapidity ($\triangle\eta_\mu$) has been determined near the edges of the LHCb detector. Figures 7(a) and 7(b) show the variation in $\triangle\eta_\mu$ at the outer edge of the detector and the edge of the detector adjacent the beam pipe. From these plots it can be seen that the detector acceptance range in pseudorapidity is $1.86 < \eta < 4.97$. These variations in $\triangle\eta_\mu$ near the detector edges have been parameterised by straight line fits to the data in the regions $1.8 < \eta < 2.5$ and $4 < \eta < 5$ and yield pseudorapidity resolutions of $(2.4 \pm 0.3)\times10^{-3}$ and $(1.4 \pm 0.6)\times10^{-3}$ at muon pseudorapidities of 1.86 and 4.97 respectively. The percentage change between the number of events where both muons lie within the ranges $1.8573 < \eta < 4.968$ and $1.8627 < \eta < 4.972$ has been taken as the systematic uncertainty on our calculated geometric acceptance. The calculated value is 0.13%.

Kinematic acceptance: The main uncertainties arising from our estimation of the kinematic acceptance are due to the accuracy of the LHCb detector simulation. The detector simulation will be tuned using data once it is available. In particular the performance of the muon sub-system can be accurately assessed using events containing J/ψ, Υ or Z particles that decay into $\mu^+\mu^-$ pairs. Once the detector simulation has been re-tuned in this way the kinematic acceptance should contribute a systematic uncertainty on the proposed luminosity measurement of better than 0.1%, as has been obtained using this procedure at other experiments [**?**].

In particular, the requirement that $P_T^{\mu\mu} < 50$ MeV/c means that any bias on the transverse momentum scale must be known to $\sim$0.1 MeV/c and (because the momentum spectrum is falling in the region of the cut) the uncertainty on the transverse momentum resolution must be known to $\sim$1 MeV/c. Given that the transverse momentum resolution on a typical signal muon is 6 MeV/c [23], such precisions should be obtainable by calibrating on muons from prompt J/ψ which have a similar momentum spectrum.

7.5 Reconstruction efficiency

As was pointed out in Section 3 the reconstruction efficiency can be determined from data and is expressible as the product of three components:

$$\varepsilon_{el}^{reco} = (\varepsilon_{trk}^{(1)} \times \varepsilon_{match}^{(1)} \times \varepsilon_{id}^{(1)}) \times (\varepsilon_{trk}^{(2)} \times \varepsilon_{match}^{(2)} \times \varepsilon_{id}^{(2)}) \tag{11}$$

We will now outline methods that will allow these terms to be measured from data. The uncertainties quoted below are estimates.

Tracking efficiency: ε_{trk} can be determined from data using a pure unbiased sample of $W \to \mu\nu$ candidate events selected using a tight set of selection criteria based on muon chamber information. The fraction of events in such a sample that have a reconstructed track that points to the appropriate muon chamber deposit will give ε_{trk}. We estimate that a measurement of ε_{trk} will have an associated systematic uncertainty of 0.4%.

Matching efficiency: The efficiency to reconstruct muon towers and match them to reconstructed tracks, ε_{match}, can be found using a data set containing events with at least one high P_T muon, for example events that pass the single muon trigger line and having $P_T > 10$ GeV/c. The muon in these events is then combined with all the opposite sign high P_T tracks in the event. If a combination has an invariant mass close to the Z mass and the track points to an active area in the muon chambers the track is considered a candidate. The fraction of these candidate tracks that are actually reconstructed offline as muons will be equal to ε_{match}. We estimate that a measurement of ε_{match} will have an associated systematic uncertainty of 0.4%.

Identification efficiency: The muon ID efficiency, ε_{id}, can be measured using a clean sample of muons that have been selected without using the cuts you wish to examine. Such a sample can be obtained from $J/\psi \to \mu\mu$ events that have passed the trigger via any stream bar the dimuon trigger stream (selecting events from the dimuon stream would bias the sample). One of the legs of the J/ψ can then be used to tag the J/ψ, while the other can be used as a probe to measure the muon efficiency. The efficiency will be equal to the number of probe muons that pass the identification cuts divided by the total number of probe muons. Assuming an identification efficiency of 99% and a sample of 10^4 muons such a measurement of ε_{id} will have an associated systematic uncertainty of 0.1%.

7.6 Trigger efficiency

The trigger efficiency, $\varepsilon_{el}^{trigger}$, of our signal process can be determined using a sample of minimum bias events that pass the trigger and contain an offline reconstructed $\mu\mu$ pair. The trigger efficiency will be equal

to the fraction of these events that have passed via the dimuon trigger stream. The uncertainty on such a determination of the trigger efficiency will depend on the size of the sample used. With 10^5 dimuon events and assuming a dimuon trigger efficiency of 44% the uncertainty will be 0.5%.

Source	Estimated systematic uncertainty (%)
Rescattering corrections	0.13
Proton EM form factors	0.3
σ_{el} prediction total	0.33
K/π mis-id	0.23
Dimuons produced via DPE	0.50
Dimuons produced via $\gamma\gamma$ fusion	0.27
Background total	0.61
Geometric acceptance	0.13
Kinematic acceptance	0.1
Acceptance total	0.16
Trigger	0.5
Tracking	0.4
Track muon chamber matching	0.4
Muon identification	0.5
Efficiency total	0.76
Total	1.04

Table 5 Estimated systematic uncertainties on a luminosity measurement at LHCb using the $pp \to p + \mu^+\mu^- + p$ channel.

7.7 Resulting measurement uncertainty

The total systematic uncertainty on a measurement of the integrated luminosity using the measured rate of $pp \to p + \mu^+\mu^- + p$ events at LHCb is therefore estimated to be 1.0%. Assuming an average instantaneous luminosity of $2 \times 10^{32}\ cm^{-2}s^{-1}$ with 1 fb^{-1} of data the following integrated luminosity measurement is expected

$$\int \mathcal{L}dt = 1 \pm 0.014(stat.) \pm 0.010(syst.) fb^{-1} \tag{12}$$

This equates to a total measurement uncertainty of 1.8%. The largest sources of uncertainty come from estimates on how well the trigger and reconstruction efficiency for muons will be known in LHCb and on the background due to to dimuons produced via double Pomeron exchange. The uncertainty on the latter is due to both the theoretical modeling of the process and the measurement uncertainties in the Pomeron flux and Pomeron parton distribution functions (PDFs) that have been determined using $H1$ and Zeus data from the Hera accelerator at DESY. Recently measurements have been made of the cross-sections for exclusive e^+e^- [24] , $\gamma\gamma$ [25] and di-jet [26] production by the CDF collaboration at the Tevatron. These measurements will further constrain the Pomeron flux and PDFs and will allow for the refinement of the theoretical models describing the double Pomeron exchange production mechanism. We thus expect

the uncertainty on the predicted cross-section of dimuons produced via DPE to be reduced in the near future which will allow for more accurate luminosity measurements at LHCb using the $pp \to p + \mu^+\mu^- + p$ process.

8 Conclusions

We expect 5210 $pp \to p + \mu^+\mu^- + p$ events to be recorded and reconstructed at LHCb in 1 fb^{-1} of data. We have proposed a set of simple offline selection criteria that will reduce the background to a level that is $(4.1 \pm 0.5(\text{stat.}) \pm 0.6(\text{syst.}))\%$ of the signal rate. This background will be dominated by the combinatoric backgrounds due to pion and kaon mis-identification, a background source that can be well understood from real data. We estimate that using the measured rate of $pp \to p + \mu^+\mu^- + p$ events in 1 fb^{-1}(2 fb^{-1}) of data, the integrated luminosity can be measured at LHCb with a $\sim 1.8\%(1.4\%)$ precision. This uncertainty is dominated by the systematic uncertainty on the predicted cross-section of dimuons produced via double Pomeron exchange and by our knowledge of the trigger and reconstruction efficiency for muons in LHCb.

9 Acknowledgements

The authors thank Mike Albrow, Valery Khoze, Alan Martin and Andrey Shamov for many useful comments and suggestions. We are particularly grateful to Andrey Shamov for providing us with a copy of his modified version of the LPAIR Monte-Carlo generator.

10 References

[1] Atlas collaboration, "Atlas forward detectors for luminosity measurement and monitoring", CERN/LHCC/2004-010, 2004.

[2] S. van der Meer, "Calibration of the effective beam height at the ISR", ISR-PO/68-31, 1968.

[3] J. Bosser et al., "LHC beam instrumentation conceptual design report", LHC Project Report 370, 2000.

[4] M. Ferro-Luzzi, "Proposal for an absolute luminosity determination in colliding beam experiments using vertex detection of beam-gas interations", CERN-PH-EP/2005-023, 2005.

[5] D. Domenici, "Detection of muons in the LHCb experiment: the aging of RPC detectors and the study of $Z \to \mu^+\mu^-$", CERN-THESIS-2007-028, 2003.

[6] M. Poli-Lener, "Triple-GEM detectors for the innermost region of the muon apparatus at the LHCb experiment", CERN-THESIS-2006-013, 2006.

[7] J. Anderson and R. McNulty, "Measuring $\sigma_Z \cdot Br(Z \to \mu^+\mu^-)$ at LHCb", LHCb note, LHCb-2007-114.

[8] V. M. Budnev et. al., "The process $pp \to ppe^+e^-$ and the possibility of its calculation by means of quantum electrodynamics only", Nucl. Phys., **B63**, 1973.

[9] A. G. Shamov and V. I. Telnov, "Precision luminosity measurement at LHC using two-photon production of $\mu^+\mu^-$ pairs.", Nucl. Instr. Meth. A494, 51, 2002.

[10] V. A. Khoze et. al., "Luminosity monitors at the LHC.", IPPP/00/01, 16 October 2000.

[11] E 140 experiment, "Measurements of the proton elastic form factors for $1GeV/c^2 \leq Q^2 \leq 3GeV/c^2$ at SLAC", Phys. Rev. **D49**, 5671, 1994.

[12] J. Vermaseren, Nucl. Phys. **B229**, 347, 1983.

[13] Private communication with K. Hennessy
K. Hennessy, "Status of studies with background", LHCb background meeting, 13 March 2008.
http://indico.cern.ch/conferenceDisplay.py?confId=3055

[14] M. Boonekamp and T. Kucs, "DPEMC: A Monte-Carlo for double diffraction", Comp. Phys. Comm. 167, 3, 2005.

[15] A. Suri and D. R. Yennie, Annals Phys. 72, 1972.

[16] A.Bialas and R.Janik, Z.Phys. C62 (1994) 487, 1994.

[17] M. Boonekamp, R. Peschanski, C. Royon, Phys. Rev. Lett. 87:251806, 2001.

[18] B. Cox and J. Forshaw, Comput. Phys. Commun.144:104, 2002.

[19] C. Royon et. al., "A global analysis of inclusive diffractive cross sections at HERA", hep-ph/0609291v2, 2006.

[20] H1 Collaboration Eur.Phys.J.C48:715-748,2006, hep-ex/0606004.

[21] J. M. Amoraal, "The J/ψ selection", LHCb-2007-052.

[22] N. Zaitsev, "The Luminosity measurement at the LHCb", LHCb note, LHCb-1998-053.

[23] J. van Tilburg, "Tracking performance in LHCb", Eur. Phys. J. C34, sup 1, 2004.

[24] CDF collaboration, "Observation of Exclusive Electron-Positron Production in Hadron-Hadron Collisions", Phys. Rev. Lett. 98, 112001, 2007.

[25] CDF collaboration, "Search for Exclusive Gamma Gamma Production in Hadron-Hadron Collisions", arXiv:0707.2374, October 2007.

[26] CDF collaboration, "Observation of Exclusive Dijet Production at the Fermilab Tevatron p-pbar Collider", arXiv:0712.0604, December 2007.